OPEN ACCESS

Seasonal trophic resource partitioning by Pacific oyster *Crassostrea gigas* and Pacific blue mussel *Mytilus trossulus* in an Alaskan estuary

Josianne Haag*, Sarah L. Mincks, Jonah Jossart, Amanda L. Kelley

College of Fisheries and Ocean Sciences, University of Alaska Fairbanks, Fairbanks, AK 99775, USA

ABSTRACT: Shellfish mariculture has expanded in Alaska, yet potential ecological interactions between cultured and native taxa have rarely been considered. Shellfish such as the Pacific oyster *Crassostrea gigas* and the Pacific blue mussel *Mytilus trossulus* are already farmed in Alaska at a small scale, with production expected to increase in coming years. *C. gigas* and *M. trossulus* selectively feed on naturally occurring particulate organic matter (POM) sources; thus, understanding the partitioning of trophic resources by these bivalves has implications for mariculture site selection and marine management. We identified temporal patterns in food source consumption by *C. gigas* and *M. trossulus* in Jakolof Bay, Alaska. We estimated endmember contributions (phytoplankton, macroalgae, terrestrial organic matter, and zooplankton) to the suspended POM pool and to the 2 bivalves using bulk stable isotopes (δ^{13}C and δ^{15}N) in April, June, August, and December 2023. While δ^{13}C values remained comparable for both bivalves across sampling periods, *C. gigas* had higher δ^{15}N values than *M. trossulus*, indicating that although both bivalves ultimately derive carbon from similar sources of primary production, *C. gigas* feeds at a higher trophic level. Mixing model results indicate that macroalgae contributed 4−58% of the assimilated carbon in *C. gigas* and 25−75% in *M. trossulus*. These results suggest that farming shellfish in areas with macroalgae populations (i.e. farmed in co-culture or wild) could offer *C. gigas* and *M. trossulus* an additional source of organic matter.

KEY WORDS: Alaska · Aquaculture · Stable isotopes · *Crassostrea gigas* · *Mytilus trossulus*

1. INTRODUCTION

Shellfish are considered one of the most sustainable mariculture products because they derive their food entirely from naturally occurring sources (Brown et al. 2020). However, shellfish farms are typically located in coastal ecosystems that also support natural populations of bivalves, and the addition of farmed shellfish risks exceeding the carrying capacity of coastal environments by depleting the available food (Dame & Prins 1997, Cranford et al. 2014). Bivalves consume a variety of complex organic compounds suspended in the water column that comprise the particulate organic matter (POM) pool, and bivalve diets can mirror variations in POM composition (Riera 2007, Xu et al. 2016). Stocking densities of farmed bivalves should be designed such that POM concentrations remain within the bounds of naturally occurring fluctuations in order to maintain energy flow and food web structure in the recipient environment (Crowder & Norse 2008). A proposed solution to minimize the effects of farmed bivalves on both the POM pool and the local food web is to co-culture bivalves with macroalgae, which also produce detritus that is exported to the surrounding environment (Xu et al. 2016). Despite the rapid expansion of the mariculture industry in the Northern Gulf of Alaska (NGA), the impact of such activities on coastal ecosystem processes has received little attention.

*Corresponding author: jhaag6@alaska.edu

The Pacific oyster *Crassostrea gigas* and the Pacific blue mussel *Mytilus trossulus* comprise half of Alaska's mariculture industry revenue (Alaska Mariculture Task Force 2018). Wild *M. trossulus* dominate the intertidal zone and provide many ecosystem services, such as stabilizing benthic substrate, transferring energy from primary producers to larger consumers, and creating habitat for other organisms (Bodkin et al. 2018, Khalaman et al. 2021). Conversely, *C. gigas* is only found in farm settings, as cold high-latitude waters inhibit natural spawning events (Castaños et al. 2009). As selective feeders, *C. gigas* and *M. trossulus* reject particles of poor nutritive value in favor of higher quality foods (Levinton et al. 2002). These bivalves consume marine phytoplankton (Cognie et al. 2001, Kasim & Mukai 2009), detrital macroalgae (Levinton et al. 2002, Emery et al. 2016), terrestrial organic matter (TOM; Christie & Bendell 2009), and zooplankton (Dupuy et al. 1999, Lehane & Davenport 2006, Kamiyama 2011). The ctenidia and labial palps of *C. gigas* select for particles >5 µm using ciliary and mucous-based processes; however, selection does not necessarily always occur at both organs (Ward et al. 1998, Rahman et al. 2020). Labial palps are the main sorting structure in *M. trossulus*, which tends to consume smaller particles than *C. gigas* (2−20 µm) because of the finer mesh size of its gill sieve (Shumway et al. 1985, Ward et al. 1998, Rahman et al. 2020). These anatomical differences can lead to species-specific differences in the fraction of POM utilized.

Co-culturing with macroalgae as a means of minimizing the environmental impacts of bivalve farming (Xu et al. 2016, Chebil Ajjabi et al. 2018, Hargrave et al. 2022) assumes that bivalves do, in fact, feed on macroalgal detritus. Macroalgae are commonly viewed as a poor food resource for many marine invertebrates due to the high content of relatively indigestible materials, such as cellulose and lignin, leaving a small fraction of carbon available for assimilation (Crosby et al. 1989, Langdon & Newell 1990). However, recent evidence indicates macroalgal detritus is the dominant source of carbon assimilated by *M. trossulus* in the NGA (Siegert et al. 2022, Corliss et al. 2024), although uptake by *C. gigas* has not been previously examined in this region. As senescing macroalgae decompose, the dissolved nitrogen released to the surrounding water is quickly assimilated by an associated microbiome colonizing the detrital particles, increasing the nutritional value of macroalgal detritus as a potential food source for invertebrates (Sosik & Simenstad 2013). Nonetheless, phytoplankton is still considered the primary food source of bivalves

based on relatively low carbon-to-nitrogen ratios (Cranford & Grant 1990, Enríquez et al. 1993).

Bulk stable isotope analysis is a powerful tool for resolving the sources of organic matter entering the food web (e.g. DeNiro & Epstein 1978, Xu & Yang 2007, Kang et al. 2009, Christie & Bendell 2009, Emery et al. 2016). Fixed carbon derived from different primary producers (phytoplankton, macroalgae, and terrestrial plants) can be differentiated based on the δ^{13}C values of each source, which are modified by the environment and by distinct photosynthetic mechanisms, providing an opportunity to determine the relative contribution of each source to the total carbon assimilated by a consumer. For example, some species of macroalgae and phytoplankton can utilize bicarbonate, which results in a higher δ^{13}C value relative to carbon dioxide (Maberly et al. 1992). By contrast, nitrogen isotope values are enriched as organic matter passes through the food web, such that the δ^{15}N value indicates the trophic position of an organism because an organism retains the heavier nitrogen isotope, ^{15}N, more readily than ^{14}N when assimilating organic matter into body tissues (Peterson & Fry 1987, Post 2002).

This study resolved the seasonal patterns in trophic resource use of *C. gigas* and *M. trossulus* in a productive bay in the NGA, where extreme seasonality requires temporal sampling to capture the variability of natural systems (Miller & Kelley 2021). We determined the contribution of various carbon sources (phytoplankton, macroalgae, TOM, and zooplankton) to the pool of suspended POM and evaluated the assimilation of organic matter derived from primary producers and zooplankton by these bivalves in a mariculture setting using bulk stable isotope analysis. Understanding the relationship between farmed shellfish and POM will not only improve our understanding of the ecology of these bivalves but will also inform sustainable practices in a state where the mariculture industry is rapidly expanding.

2. MATERIALS AND METHODS

2.1. Study area

Jakolof Bay (59.5569° N, 151.5103° W) is located in the southern part of Kachemak Bay in Southeastern Cook Inlet, Alaska (Fig. 1). The bay experiences a maximum tidal range of 8 m during spring tides (Archer 2013) and a water residence time of less than 1 d, which allows for high nutrient loading from offshore water and submarine groundwater discharge (Haag et al. 2023). As a result, productivity is elevated
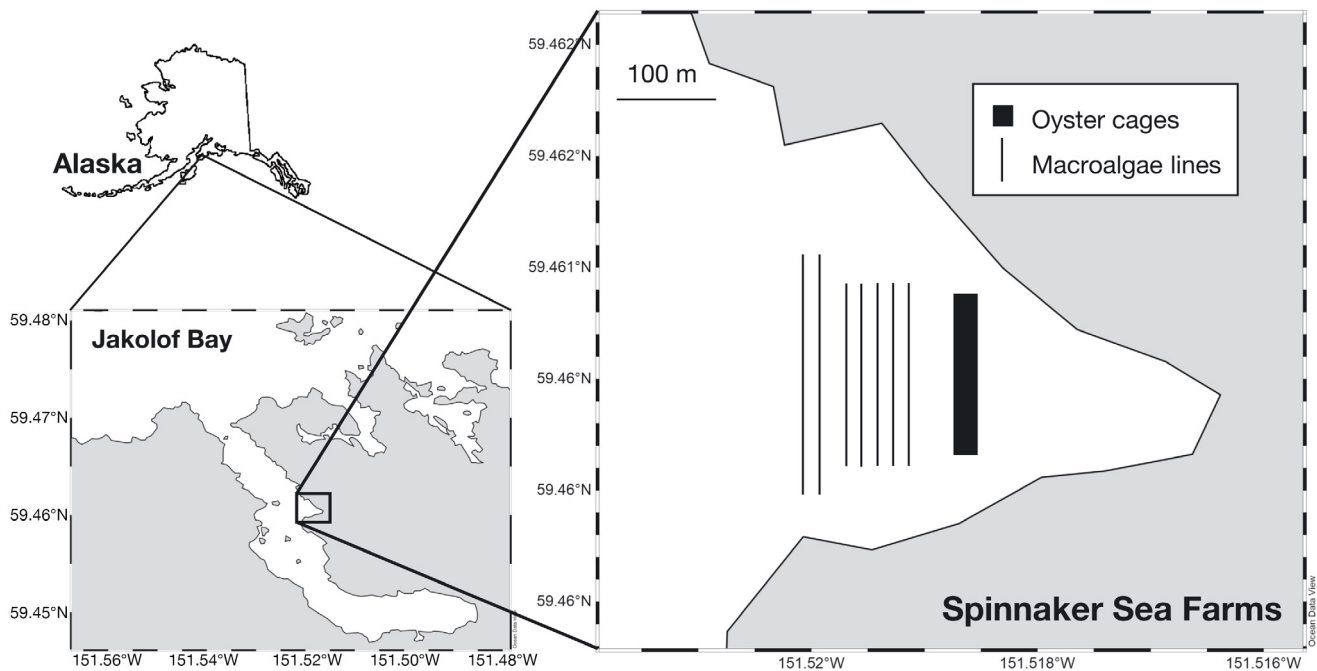
Fig. 1. Study area sampled during April, June, August, and December 2023. The Pacific oyster *Crassostrea gigas* cages at Spinnaker Sea Farms are located closer to the shoreline than the longlines of sugar kelp *Saccharina latissima* and ribbon kelp *Alaria marginata*

compared to larger or deeper bays and supports dense beds of macroalgae covering much of the seafloor. Offshore water transport can also deliver a high abundance of zooplankton following the spring bloom (Stabeno et al. 2004, Strom et al. 2019), although the zooplankton assemblage of Lower Cook Inlet reaches a maximum in June when it is mainly composed of meroplanktonic larvae (McKinstry et al. 2022). Given this high productivity as well as relative accessibility, Jakolof Bay is home to at least 3 active oyster farms, including Spinnaker Sea Farms (59.4603° N, 151.5190° W), a small-scale farm located in a protected cove approximately halfway into Jakolof Bay with a mean depth of 5.5 m at lower low tide (Fig. 1).

Shellfish farmers first introduced *C. gigas* to Jakolof Bay in the early 1990s, housing them in lantern nets and metal cages suspended in the water column. This species cannot reproduce in southcentral Alaska's cold waters, so it remains restricted to mariculture activities (Castaños et al. 2009). Spinnaker Sea Farms grows long lines of *C. gigas*, as well as sugar kelp *Saccharina latissima* and ribbon kelp *Alaria marginata*. The growing season for macroalgae extends from October to April; therefore, any contribution of macroalgae to the POM pool outside of that timeframe may come from wild growth on the seafloor and biofouling on the mariculture structures.

2.2. Sample collection

We obtained farmed adult *C. gigas* as well as naturally occurring *M. trossulus* from the Spinnaker Sea Farms site on 21 April, 18 June, 19 August, and 6 December 2023 to capture seasonal variability. A total of 30 individuals of *M. trossulus* from juvenile to adult were collected haphazardly from within 10 m of the farm by scraping the intertidal rocks and farm structures. Individuals of *C. gigas* (n = 7—30, depending on availability) were purchased from Spinnaker Sea Farms in each sampling period. The specimens were transported live to either the Kasitsna Bay Laboratory or Kachemak Bay National Estuarine Research Reserve and cleaned to remove epifauna. Live animals were maintained in filtered seawater, facilitating the evacuation of fecal contents prior to tissue sampling. Within 3 d of collection, we measured shell length, width, and height (mm) before dissecting the specimens to remove the adductor muscles for bulk carbon and nitrogen stable isotope analysis. The assimilation time of this tissue is on the order of 1—2 wk (8.5 d for carbon and 14.5 d for nitrogen; Dubois et al. 2007), ensuring that sufficient change in bulk stable isotopes can be observed through seasonal sampling. For both bivalves, the adductor muscle lacks lipids (C:N ratio: 3.56 ± 0.38 and 3.31 ± 0.12 for *C. gigas* and *M. trossulus*, respectively), allowing us

to forgo lipid extraction, thus simplifying the processing steps (Post et al. 2007, Yokoyama et al. 2008). Shells were oven-dried for 1 wk at 50°C and weighed. As all shell size metrics were highly correlated, only shell weight was used in further analyses (Fig. A1 in the Appendix).

We identified 4 potentially important food source endmembers: phytoplankton, macroalgae, TOM, and zooplankton, and estimated the relative contribution of each of these to POM. In practice, bivalves ingest suspended POM that potentially comprises all these sources as well as bacteria, but they have the capacity to select desirable particles from this pool (Ward & Shumway 2004). Triplicate water samples for suspended POM were collected at the farm site during each field collection to estimate the available contribution of each potential carbon source to the POM pool and the bivalves. Water samples (2 l) were first filtered through 153 µm mesh to eliminate large zooplankton and then vacuum-filtered through a 0.47 µm GF/F Whatman filter to collect smaller particulates; the filters were subsequently oven-dried.

We adopted the strategy of McMahon et al. (2021) for the phytoplankton endmember: using a 153 µm plankton net around the farm site, we collected individual copepods of various taxa including *Pseudocalanus* spp. and *Acartia* spp. and applied a trophic discrimination factor to the copepod stable isotope values to calculate the isotope signature of their phytoplankton diet (Δ^{13}C: 0.4‰; Δ^{15}N: 3.4‰; Post 2002). This strategy assumed that copepods selectively feed on phytoplankton and therefore can be related to their phytoplankton diet by applying a discrimination factor (Calbet & Landry 2004). In June, we also hand-picked chain-forming diatoms from the net-collected plankton to validate the stable isotope signature of the phytoplankton endmember that was calculated by applying the trophic discrimination factor to the copepod signature, as diatoms dominate the phytoplankton assemblage in the nearshore of this region throughout most of spring and summer (Strom et al. 2006).

We also utilized the original copepod stable isotope values to represent the zooplankton endmembers. Zooplankton endmembers are not typically included in studies such as this (Dubois et al. 2007, Riera 2007, Emery et al. 2016, Park et al. 2021); however, the bivalve stable isotope data suggested feeding above the level of the primary producers, so the copepod endmember was included to represent a primary consumer group as a possible bivalve food source. Zooplankton samples were preserved in 70% isopropyl alcohol. Individual copepods were then selected using a dissecting microscope, rinsed in deionized water, and dried prior to analysis.

We collected the dominant macroalgae and potential sources of TOM by hand in each season from the intertidal zone or from biofouling at the farm site. We sampled the blades of *Fucus distichus* and *Ulva lactuca* in every season, *S. latissima* and *Pylaiella littoralis* in June and August, *A. marginata* in every season but December, *Nereocystis luekteana* in August and December, and *Halosaccion glandiforme* in August. We collected Sitka spruce *Picea sitchensis* needles in every season, moss in every season but June, grass in every season but December, and *Alnus* sp. leaves in every season but April. We observed a massive deposition of *P. sitchensis* pollen in June that appeared as a slick on the sea surface in Jakolof Bay, as is common for this region. We thus included a pollen sample as an endmember for that sampling period, which was obtained by collecting triplicate 100 ml surface-water samples where concentrated pollen was observed and filtering according to the protocol for POM samples.

2.3. Bulk stable isotope analysis

Adductor muscle tissue samples from *C. gigas* and *M. trossulus* were frozen and stored at −80°C. No lipid extraction was performed, as lipid removal does not change the δ^{13}C or δ^{15}N values of muscle tissue (Yokoyama et al. 2008). All source endmember samples and POM samples were desiccated at 50°C for over 24 h. The copepod samples, diatom samples, and POM filters were exposed to HCl vapor for 24 h to remove inorganic (carbonate) carbon (Harris et al. 2001). Samples were homogenized to a powder and measured at the Alaska Stable Isotope Facility at the University of Alaska Fairbanks using a Thermo Scientific Conflo IV™ interfaced with a Thermo Scientific DeltaV^Plus Mass Spectrometer™. Values are expressed in delta notation in parts per thousand (‰) using standards of Vienna Pee Dee Belemnite for δ^{13}C and atmospheric N_2 for δ^{15}N. The instrument's standard deviation was 0.10‰ for δ^{13}C and 0.16‰ for δ^{15}N (n = 28).

2.4. Data analysis

Statistical tests were performed in R (v.4.3.1). To test for seasonal variation in stable-isotope ratios of endmembers, POM, and bivalves, normality and homoscedasticity were first checked using Shapiro-Wilk and Levene's tests, respectively. If normality

was found, differences between groups were tested using ANOVA (α = 0.05) followed by a post-hoc Tukey honestly significant difference (HSD) test (α = 0.05) with the Bonferroni correction. If normality was not found, a Kruskal-Wallis test (α = 0.05) was conducted, followed by a post-hoc Dunn's test (α = 0.05). To determine if seasonal differences in bulk stable isotopes were related to the size of the bivalves, we produced Pearson correlations (α = 0.05) between stable isotope values of the bivalves and shell dry weight.

We determined the relative contributions of taxonomically similar pooled source endmembers of phytoplankton, macroalgae, TOM, and zooplankton as food sources for *C. gigas* and *M. trossulus* by performing a stable isotope mixing model under a Bayesian framework for each season (Stock et al. 2018). We ran MIXSIAR (v.3.1.12; Stock & Semmens 2016) in R using functional JAGS (www.sourceforge.net/projects/mcmc-jags/files). No priors were used. Dubois et al. (2007) provided the trophic discrimination factors used in the model for both bivalves: $\Delta^{13}C = 1.85 \pm 0.19‰$, $\Delta^{15}N = 3.79 \pm 0.19‰$ for *C. gigas;* and $\Delta^{13}C = 2.17 \pm 0.32‰$, $\Delta^{15}N = 3.78 \pm 0.29‰$ for *M. trossulus*. The model ran at 1 000 000 iterations (burn-in: 500 000; chains: 3) and results were diagnosed using the Gelman-Rubin Diagnostic and the Geweke Diagnostic. We used a Z-score (α = 0.05) to compare the proportions of each endmember for *C. gigas*, *M. trossulus*, and POM. We adjusted the p-values of this test with the Bonferroni correction method.

3. RESULTS

The endmembers were well separated in the $\delta^{13}C$ and $\delta^{15}N$ isotope space (Table 1, Fig. 2). Macroalgal $\delta^{13}C$ values ranged from −22.54 to −14.59‰, and $\delta^{15}N$ values ranged from 3.70 to 11.22‰ (Table 1). Mean macroalgal $\delta^{13}C$ values did not vary seasonally (ANOVA, $F = 0.6$, df = 3, p = 0.625), whereas mean macroalgal $\delta^{15}N$ was significantly different in December than in June and August (Tukey's HSD, p < 0.0328). TOM sources exhibited the greatest variation in both stable isotopes, with $\delta^{13}C$ values ranging from −32.29 to −23.49‰ and $\delta^{15}N$ values ranging from −1.74 to 13.55‰ (Table 1), yet mean TOM stable isotope values did not differ among time points (Dunn's test, p > 0.0603). The copepods (i.e. zooplankton endmember) displayed $\delta^{13}C$ values ranging from −24.74 to −17.64‰ and $\delta^{15}N$ values ranging from 7.54 to 13.26‰ (Table 1). Copepod $\delta^{13}C$ and $\delta^{15}N$ values did not differ among seasons ($\delta^{13}C$-specific

Table 1. Mean (±SD) $\delta^{13}C$ and $\delta^{15}N$ of *Crassostrea gigas*, *Mytilus trossulus*, particulate organic matter, and endmembers sampled on 21 April, 18 June, 19 August, and 6 December 2023. Sample sizes denoted in parentheses when n > 1

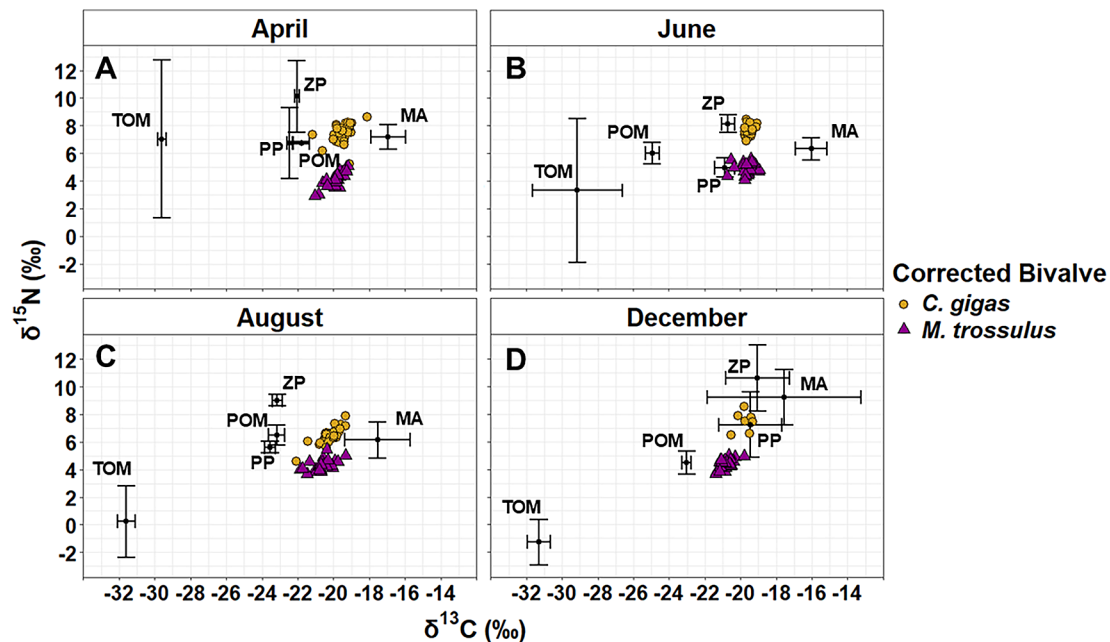|	April $\delta^{13}C$ (‰)	April $\delta^{15}N$ (‰)	June $\delta^{13}C$ (‰)	June $\delta^{15}N$ (‰)	August $\delta^{13}C$ (‰)	August $\delta^{15}N$ (‰)	December $\delta^{13}C$ (‰)	December $\delta^{15}N$ (‰)
C. gigas	−17.65 ± 0.55 (30)	11.28 ± 0.70 (30)	−17.67 ± 0.18 (27)	11.45 ± 0.39 (27)	−18.36 ± 0.57 (30)	10.21 ± 0.60 (30)	−17.92 ± 0.43 (7)	11.24 ± 0.72 (7)
M. trossulus	−17.72 ± 0.43 (30)	7.91 ± 0.50 (30)	−17.47 ± 0.39 (30)	8.64 ± 0.41 (30)	−18.46 ± 0.54 (30)	8.11 ± 0.38 (30)	−18.67 ± 0.33 (30)	8.18 ± 0.34 (30)
Particulate organic matter	−21.80 ± 0.45 (3)	6.75 ± 0.09 (3)	−24.93 ± 0.39 (3)	6.01 ± 0.77 (3)	−23.17 ± 0.46 (3)	6.48 ± 0.73 (3)	−23.02 ± 0.27 (3)	4.47 ± 0.84 (3)
Copepods (i.e. zooplankton)	−22.05 ± 0.14 (3)	10.11 ± 2.57 (3)	−20.69 ± 0.36 (3)	8.14 ± 0.63 (3)	−23.15 ± 0.29 (3)	9.02 ± 0.44 (3)	−19.04 ± 1.78 (3)	10.62 ± 2.38 (3)
Estimated phytoplankton	−22.45 ± 0.14 (3)	6.71 ± 2.57 (3)	−20.85 ± 0.56 (3)	4.97 ± 0.69 (3)	−23.55 ± 0.29 (3)	5.62 ± 0.44 (3)	−19.44 ± 1.78 (3)	7.22 ± 2.37 (3)
Chained diatoms			−20.13	5.66				
Macroalgae	−16.94 ± 0.96 (3)	7.16 ± 0.88 (3)	−16.02 ± 0.88 (5)	6.32 ± 0.79 (5)	−17.52 ± 1.83 (8)	6.14 ± 1.32 (8)	−17.55 ± 4.32 (3)	9.21 ± 2.02 (3)
Alaria marginata	−17.1	6.53	−16.44	5.24	−18.43	3.70		
Halosaccion glandiforme					−14.60	5.84		
Fucus distichus	−15.90	6.79	−15.94	6.5	−16.19	6.61		
Nereocystis luetkeana					−18.23	5.12	−15.16	7.18
Pylaiella littoralis			−16.96	6.72	−19.40	7.42	−22.54	11.22
Saccharina latissima			−14.59	5.86	−16.87 ± 1.80 (2)	6.27 ± 0.15 (2)		
Ulva lactuca	−17.81	8.17	−16.15	7.28	−19.56	7.91	−14.95	9.22
Terrestrial organic matter	−29.60 ± 0.24 (3)	7.03 ± 5.70 (3)	−29.14 ± 2.52 (3)	3.30 ± 5.22 (3)	−31.59 ± 0.48 (4)	0.22 ± 2.60 (4)	−31.30 ± 0.65 (3)	−1.27 ± 0.45 (3)
Moss	−29.33	4.54			−31.21	−0.17	−30.56	−1.5
Picea sitchensis needles	−29.72	2.99	−31.03	6.58	−32.29	−1.20	−31.82	−0.75
P. sitchensis pollen			−29.00 ± 0.25 (3)	−0.32 ± 0.24 (3)				
Grass	−29.76	13.55	−24.74	12.44	−31.40	4.00		
Alnus sp. leaves			−32.07	1.76	−31.46	−1.74	−31.50	−1.56

Fig. 2. $\delta^{13}C-\delta^{15}N$ biplots for *Crassostrea gigas* and *Mytilus trossulus* on (A) 21 April 21, (B) 18 June, (C) 19 August, and (D) 6 December 2023 in Jakolof Bay. The potential food sources, which are taxonomically pooled (PP: phytoplankton; MA: macroalgae; TOM: terrestrial organic matter; ZP: zooplankton), and the particulate organic matter (POM) are represented by a mean and standard deviation. The bivalve values were adjusted for trophic discrimination using values from Dubois et al. (2007)

Tukey's HSD, p > 0.2097; $\delta^{15}N$-specific Kruskal-Wallis, p = 0.1580), except for copepod $\delta^{13}C$ values between April and December (Tukey's HSD, p = 0.0175).

The $\delta^{13}C$ copepod-derived phytoplankton endmember was comparable to the lone phytoplankton sample (Table 1, Fig. 2). Applying a trophic discrimination factor to the isotopic value for copepods yielded an estimated value for phytoplankton ($\delta^{13}C$: −20.25 ± 0.49‰; $\delta^{15}N$: 4.77 ± 0.88‰) that agreed well with the single sample of diatom chains collected in the same sampling period ($\delta^{13}C$: −20.13‰; $\delta^{15}N$: 5.66‰), validating the use of this approach to estimate the phytoplankton signature (Table 1). Given that phytoplankton values were calculated from the copepod values, the same seasonal pattern was observed with differences in $\delta^{13}C$ only between April and December (Tukey's HSD, p = 0.0134).

Isotope ratios for POM, *C. gigas*, and *M. trossulus* fell within the isotopic space of the endmembers (Fig. 2). The $\delta^{13}C$ of POM differed among seasons (Tukey's HSD, p < 0.024), except between August and December (Tukey's HSD, p = 0.966), indicating that the composition of POM varied seasonally. The $\delta^{15}N$ of POM remained consistent through most of the seasons (Tukey's HSD, p > 0.088), although it was significantly lower in December than in April or August (Tukey's HSD, p < 0.027). The $\delta^{13}C$ values for both bivalves were similar to each other at each time point

(Dunn's test, p > 0.079), and both differed between April/June and August/December, suggesting similar patterns of organic-matter consumption (Fig. 3). However, $\delta^{15}N$ values were consistently higher in *C. gigas* than in *M. trossulus* across all sampling periods (Dunn's test, p < 0.0001; Fig. 3), suggesting that *C. gigas* fed at a higher trophic level. The difference in $\delta^{15}N$ between species ranged from 2.81 ± 0.56 to 3.37 ± 0.86‰, roughly equivalent to one trophic level difference. No significant relationships existed between the stable isotope values for each bivalve and shell dry weight (Pearson correlation, F = 0.979−2.181, df = 92−118, p > 0.142) apart from mussel $\delta^{13}C$ being poorly correlated with shell dry weight (R^2 = −0.240, Pearson correlation, F = 7.19, df = 118, p = 0.008). The lack of relationship between bulk stable isotopes and shell weight suggests that seasonal differences in $\delta^{13}C$ and $\delta^{15}N$ values are attributable to differences in diet, not body size.

Mixing model results also indicated seasonal differences in POM composition and in the resource use of *C. gigas* and *M. trossulus* (Table A1, Fig. 4). Phytoplankton was the largest contributor to POM composition in April, August, and December (Z-score, p < 0.012). Zooplankton comprised the largest proportion of POM in June, followed closely by TOM (Z-score, p < 0.001). Macroalgae was the primary carbon source of both bivalves in August, even when the proportion of
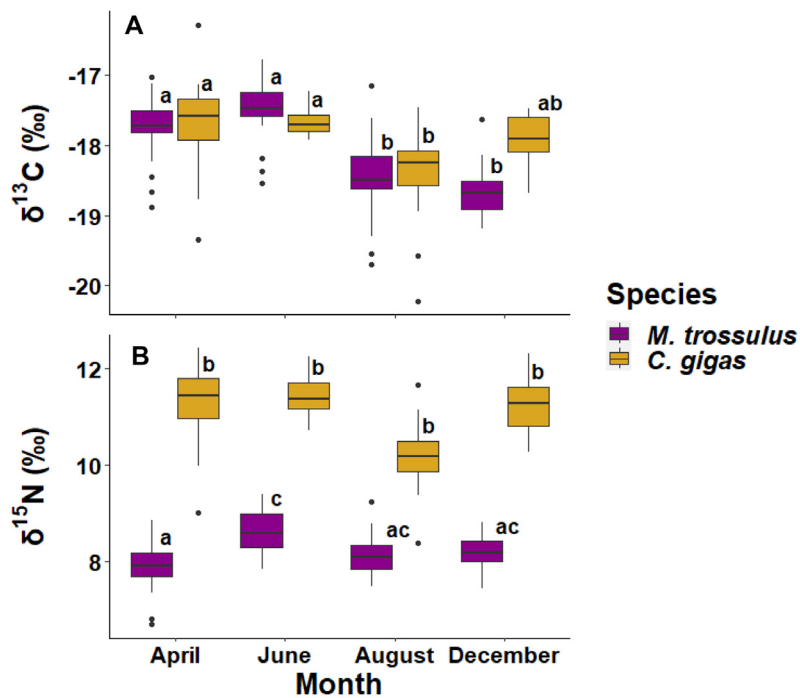
Fig. 3. (A) $\delta^{13}C$ and (B) $\delta^{15}N$ signatures of *Crassostrea gigas* and *Mytilus trossulus* from Jakolof Bay over 4 time periods in 2023. Bolded horizontal line: median; boxes: 25th—75th percentile range (IQR); whiskers: max./min. values ≤1.5 × IQR above / below box; dots: outliers. Different lowercase letters indicate significant differences according to Tukey's HSD or Dunn's test (α = 0.05)

macroalgae in POM was negligible (*Z*-score, p < 0.001). Phytoplankton was favored by *M. trossulus* in all other seasons (*Z*-score, p < 0.015), while *C. gigas* consumed predominantly macroalgae in April and August, zooplankton in June, and phytoplankton in December

(*Z*-score, p < 0.001). TOM played a negligible role in the resource use of *C. gigas* across all 4 time periods, and zooplankton was minimally consumed by *M. trossulus* (Fig. 4).

4. DISCUSSION

In contrast to the common assumption that marine invertebrates rely primarily on phytoplankton as a food source, we found that both the Pacific oyster *Crassostrea gigas* and the blue mussel *Mytilus trossulus* assimilated high proportions of macroalgal carbon into their tissues despite low proportions of macroalgae in the bulk POM pool. Bulk stable isotopes also revealed that *C. gigas* systematically maintained a higher trophic position relative to *M. trossulus* across all seasons. Zooplankton availability may thus provide a critical food resource for farmed shellfish, with potential food-web impacts on ecosystems around farm sites. Macroalgae, whether natural or farmed, could also provide an additional resource for farmed bivalves. The seasonal dynamics of zooplankton and macroalgal detritus may be important when determining appropriate locations for mariculture activities.
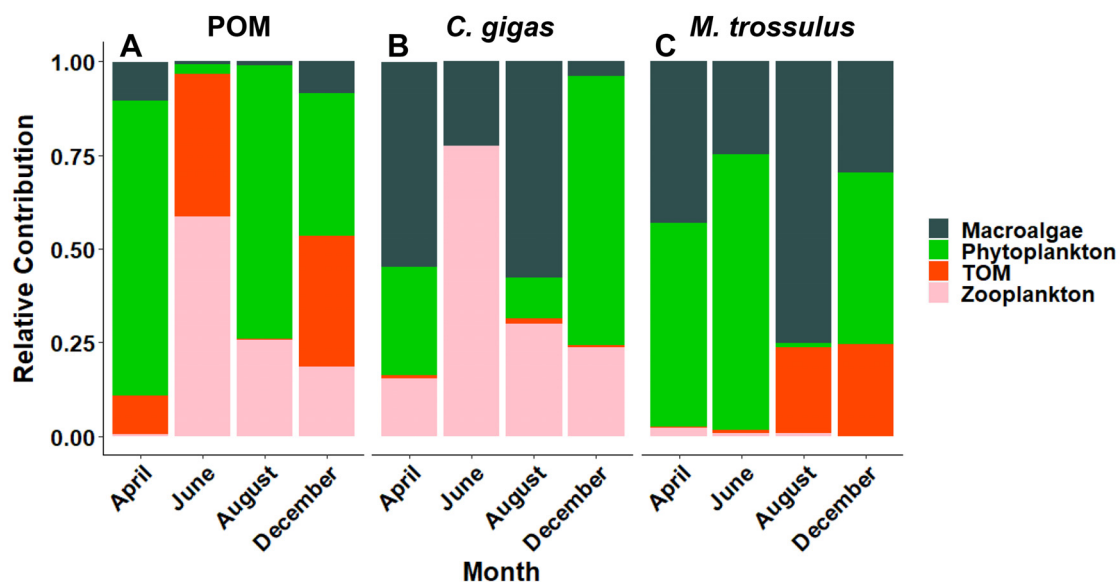

Fig. 4. Proportion of endmember contributions to (A) the particulate organic matter (POM) pool and the resource use of (B) *Crassostrea gigas* and (C) *Mytilus trossulus* across the study period in Jakolof Bay. TOM: terrestrial organic matter

Throughout the seasons, *C. gigas* and *M. trossulus* incorporated multiple food sources, including a disproportionately larger macroalgal subsidy than was present in the POM throughout most time points (Fig. 4). Except for *C. gigas* in December, both bivalves exhibited higher proportions of macroalgal carbon in their adductor muscle tissues than was present in the POM sample, suggesting that *C. gigas* and *M. trossulus* preferentially selected for detrital macroalgae. Macroalgae is largely considered a less nutritive source of food than phytoplankton, but its associated microbiome may increase its nutritional value (Sosik & Simenstad 2013, Both et al. 2020). Previous studies have shown that the diet of *M. trossulus* varies across the NGA, with macroalgal contributions ranging from 38.0 to 96.3% (Siegert et al. 2022, Corliss et al. 2024), which roughly corresponds to the range reported here (24.8–75.4%). The proportion was somewhat lower for *C. gigas* (4.0–57.8%), which is comparable to values reported in other regions (5–56%; Dubois et al. 2007, Xu & Yang 2007, Emery et al. 2016). The macroalgal endmember used in this study included live macroalgal tissue rather than the degraded material that would typically be digested by shellfish. With degradation, the δ^{13}C and δ^{15}N values of the macroalgae become more depleted (Hill & McQuaid 2009). Thus, the detrital macroalgal endmember signature may move closer within isotopic space to aquatic animal tissues presented in our study (Fig. 2). As a result, our estimate of macroalgae diet consumption for *C. gigas* and *M. trossulus* in this study may be an underestimate. In short, this study demonstrated the utilization of macroalgae by both *C. gigas* and *M. trossulus* throughout most of the year, indicating that the presence of farmed or natural macroalgae may contribute as a food subsidy for farmed shellfish.

Co-culturing shellfish and macroalgae (i.e. integrated multi-trophic aquaculture, IMTA) is suggested to enhance the productivity of each cultured species and alleviate any possible impacts of increased detritus inputs to surrounding waters (Xu et al. 2016, Chebil Ajjabi et al. 2018, Hargrave et al. 2022). A basic assumption of IMTA including *C. gigas* is that shellfish consume macroalgae detritus, but this assumption had yet to be tested in this region prior to this study. While farmed shellfish do appear to consume macroalgal carbon, other factors must also be considered in determining whether co-culturing could alleviate the potential pressures of farmed species on the natural POM pool. For example, shellfish remain in Alaskan waters year-round, whereas macroalgae like *Saccharina latissima* and *Alaria marginata* are outplanted in the fall and early winter and are harvested

in spring before biofouling occurs, which coincides with cold temperatures that decrease bivalve growth (Brown 1988, Stekoll et al. 2021). However, there are currently no estimates in the NGA for the residence time of detritus of farmed kelp in the POM pool or for the export of particulate material due to fragmentation of farmed kelp caused by physical disturbance such as storms and wave energy or bacterial degradation; it may be that detritus from farmed *S. latissima* and *A. marginata* remain in the water column long past harvest (Krumhansl & Scheibling 2012). Alternatively, interest in farming *Macrocystis pyrifera* has been growing in recent years. This macroalga achieved the most success when outplanted in February and harvested in August (Stekoll et al. 2021) and therefore may be a more suitable candidate to subsidize shellfish diet when grown in co-culture. This study did not provide clear evidence of the origin of the macroalgal detritus consumption by *C. gigas* and *M. trossulus* — whether by farmed or natural sources — or investigate how different macroalgal species may differ in their nutritional content profiles or palatability. Furthermore, we did not identify the specific macroalgal species consumed by *C. gigas*, although it is likely that the macroalgal detritus available in the water column is dominated by *S. latissima*, one of the farmed species, given that a wild population covers the entire benthos of the bay. The dominant macroalgal species present during each timepoint represented the macroalgal endmember despite nutritional and slight isotopic differences amongst taxa (i.e. red, brown, and green; Corliss et al. 2024). However, the red, brown, and green macroalgae collected in this study grouped together in isotopic space, separate from the other primary producer endmembers (Table 1, Fig. 2), suggesting that this generalization is reasonable.

The population of *C. gigas* and *M. trossulus* sampled in Jakolof Bay exhibited trophic niche partitioning, with *C. gigas* relying heavily on zooplankton, particularly in June. Nitrogen isotope values indicated roughly one trophic level difference (~2.8–3.4‰) between the 2 bivalves (Table 1, Fig. 3), in contrast to previous studies that reported much smaller differences (<1‰; Dubois et al. 2007, Riera 2007, Park et al. 2021). Consumption of zooplankton by *C. gigas* throughout the summer (Fig. 4) was not observed in *M. trossulus*, even though both bivalves are known to consume microzooplankton (Lehane & Davenport 2006, Kamiyama 2011). Gut analyses of *C. gigas* in northern Japan indicate that *C. gigas* consumes various kinds of zooplankton, typically microzooplankton including tintinnid ciliates, *Dinophysis* spp., and metazoans (copepods, copepod nauplii, and bivalve larvae) (Kamiyama

2011). However, stable isotope analysis cannot identify the specific species associated with the zooplankton endmember, particularly given the seasonal shift in the zooplankton community in this region (Both et al. 2020, McKinstry et al. 2022).

An additional caveat of the stable isotope method is acquiring a pure phytoplankton endmember. Most studies use POM samples obtained by filtering water onto a glass fiber filter as a phytoplankton endmember (Siegert et al. 2022, Corliss et al. 2024), but this method likely captures a mixture of phytoplankton as well as other detrital particles, bacteria, and even small zooplankton. Some studies argue that offshore POM samples represent a 'clean' phytoplankton sample (Miller & Page 2012), but such samples are also not representative of the nearshore phytoplankton assemblage. Cultured phytoplankton can be used (Duggins et al. 1989), but again it is difficult to represent the natural phytoplankton assemblage in the environment with the added issue of different sources of carbon (carbon dioxide and bicarbonate) and different availability of carbon isotope ratios. Due to the difficulty associated with isolating a pure phytoplankton endmember sample from other suspended particulates, we adopted the strategy of McMahon et al. (2021) to collect copepods and deduct one discrimination factor from its stable isotope values under the assumption that copepods primarily consume phytoplankton (Calbet & Landry 2004), which introduces its own bias. The phytoplankton endmember, as well as the other endmembers included in the mixing models, are the best stable isotope estimates we can derive given our resources.

The proportional assimilation of zooplankton in *C. gigas* over time mirrors the contribution of zooplankton to the POM pool, although the assemblage of zooplankton likely changed across sampling periods. The assimilation time of bulk stable isotopes into bivalve tissues can create a lag between resources in POM appearing in the bivalve adductor muscle on the order of 1–2 wk (Dubois et al. 2007). Still, the proportion of zooplankton-derived carbon in *C. gigas* matched what was available in the POM pool in every sampling period except for June, when the proportion exceeded that of POM, suggesting *C. gigas* actively selected for zooplankton in June. While there was no size difference in *C. gigas* across sampling periods, they were larger than *M. trossulus*, indicating that the disparity in zooplankton consumption was likely an artifact of gill sieve size (Shumway et al. 1985, Ward et al. 1998, Rahman et al. 2020). The zooplankton community in this region begins with a winter copepod assemblage, followed by forage fish ichthyoplankton and several large calanoid copepods emerging in March, shifting to mainly meroplankton in summer, and to gelatinous zooplankton and warm water copepods in fall (McKinstry et al. 2022). *C. gigas* may be selectively consuming zooplankton during the period when meroplanktonic larvae dominate, although future research should seek to identify the zooplankton species consumed by *C. gigas*. In Lima Bay, Croatia, the meroplanktonic larvae of the native flat oyster *Ostea edulis* contributed to 86.2% of the *C. gigas* diet, indicating that *C. gigas* is capable of larviphagy (Ezgeta-Balić et al. 2020). At the end of 2023, the *C. gigas* inventory in Jakolof Bay was 975 745 individuals, which included shellfish from seed to market size (Alaska Department of Fish and Game pers. comm.). Assuming the filtration rate of *C. gigas* varies from 0.2 to 8 l h^{-1} depending on size (Bougrier et al. 1995, Ren et al. 2000) and a bay volume of 989 000 000 l (Haag et al. 2023), 9.7% of the bay could be filtered daily by *C. gigas*. Monitoring the effect of *C. gigas* on local zooplankton communities, particularly the meroplanktonic larvae, may be crucial to coastal management as mariculture efforts continue to grow in the NGA.

5. CONCLUSIONS

Macroalgae provides a key source of organic carbon to *Crassostrea gigas* and *Mytilus trossulus* in a macroalgae-dominated bay in the NGA. As the mariculture industry in Alaska expands, so does the potential for farmed bivalves to reach carrying capacity in recipient nearshore ecosystems. Therefore, including macroalgae in farming efforts conjoined with *C. gigas* and *M. trossulus* may reduce the pressure of farmed shellfish on natural resources. Furthermore, the trophic level difference between the bivalves, combined with the dominance of zooplankton in the diet of *C. gigas*, highlights the ecological novelty that farmed *C. gigas* brings to the region and demonstrates that zooplankton provide a link between primary production and an economically important shellfish. Future research should investigate the dynamics between zooplankton and the expanding *C. gigas* industry through both the lens of aquatic farm site selection and coastal management of marine ecosystems.

LITERATURE CITED

Alaska Mariculture Task Force (2018) Alaska Mariculture Development Plan. State of Alaska, March 23, 2018. https://www.adfg.alaska.gov/Static/fishing/pdfs/mariculture/ak_mariculture_devplan_06-29-18.pdf

Archer AW (2013) World's highest tides: hypertidal coastal systems in North America, South America and Europe. Sediment Geol 284–285:1–25

Bodkin JL, Coletti HA, Ballachey BE, Monson DH, Esler D, Dean TA (2018) Variation in abundance of Pacific blue mussel (*Mytilus trossulus*) in the Northern Gulf of Alaska, 2006–2015. Deep Sea Res II 147:87–97

Both A, Byron CJ, Costa-Pierce B, Parrish CC, Brady DC (2020) Detrital subsidies in the diet of *Mytilus edulis*; macroalgal detritus likely supplements essential fatty acids. Front Mar Sci 7:561073

Bougrier S, Geairon P, Deslous-Paoli JM, Bacher C, Jonquières G (1995) Allometric relationships and effects of temperature on clearance and oxygen consumption rates of *Crassostrea gigas* (Thunberg). Aquaculture 134:143–154

Brown JR (1988) Multivariate analyses of the role of environmental factors in seasonal and site-related growth variation in the Pacific oyster *Crassostrea gigas.* Mar Ecol Prog Ser 45:225–236

Brown AR, Lilley M, Shutler J, Lowe C and others (2020) Assessing risks and mitigating impacts of harmful algal blooms on mariculture and marine fisheries. Rev Aquacult 12:1663–1688

Calbet A, Landry MR (2004) Phytoplankton growth, microzooplankton grazing, and carbon cycling in marine systems. Limnol Oceanogr 49:51–57

Castaños C, Pascual M, Camacho AP (2009) Reproductive biology of the nonnative oyster, *Crassostrea gigas* (Thunberg, 1793), as a key factor for its successful spread along the rocky shores of northern Patagonia, Argentina. J Shellfish Res 28:837–847

Chebil Ajjabi L, Abaab M, Segni R (2018) The red macroalga *Gracilaria verrucosa* in co-culture with the Mediterranean mussels *Mytilus galloprovincialis*: productivity and nutrient removal performance. Aquacult Int 26:253–266

Christie JC, Bendell LI (2009) Sources of dietary cadmium to the Pacific oyster *Crassostrea gigas.* Mar Environ Res 68:97–105

Cognie B, Barillé L, Rincé Y (2001) Selective feeding of the oyster *Crassostrea gigas* fed on a natural microphytobenthos assemblage. Estuaries 24:126–134

Corliss K, von Biela V, Coletti H, Bodkin J, Esler D, Iken K (2024) Relative importance of macroalgae and phyto-

plankton to nearshore consumers and growth across climatic conditions in the northern Gulf of Alaska. Estuaries Coasts 47:1579–1597

Cranford PJ, Grant J (1990) Particle clearance and absorption of phytoplankton and detritus by the sea scallop *Placopecten magellanicus* (Gmelin). J Exp Mar Biol Ecol 137:105–121

Cranford PJ, Duarte P, Robinson SM, Fernández-Reiriz MJ, Labarta U (2014) Suspended particulate matter depletion and flow modification inside mussel (*Mytilus galloprovincialis*) culture rafts in the Ría de Betanzos, Spain. J Exp Mar Biol Ecol 452:70–81

Crosby MP, Langdon CJ, Newell RIE (1989) Importance of refractory plant material to the carbon budget of the oyster *Crassostrea virginica.* Mar Biol 100:343–352

Crowder L, Norse E (2008) Essential ecological insights for marine ecosystem-based management and marine spatial planning. Mar Policy 32:772–778

Dame RF, Prins TC (1997) Bivalve carrying capacity in coastal ecosystems. Aquat Ecol 31:409–421

DeNiro MJ, Epstein S (1978) Influence of diet on the distribution of carbon isotopes in animals. Geochim Cosmochim Acta 42:495–506

Dubois S, Jean-Louis B, Bertrand B, Lefebvre S (2007) Isotope trophic-step fractionation of suspension-feeding species: implications for food partitioning in coastal ecosystems. J Exp Mar Biol Ecol 351:121–128

Duggins DO, Simenstad CA, Estes JA (1989) Magnification of secondary production by kelp detritus in coastal marine ecosystems. Science 245:170–173

Dupuy C, Le Gall S, Hartmann HJ, Bréret M (1999) Retention of ciliates and flagellates by the oyster *Crassostrea gigas* in French Atlantic coastal ponds: protists as a trophic link between bacterioplankton and benthic suspension-feeders. Mar Ecol Prog Ser 177:165–175

Emery KA, Wilkinson GM, Camacho-Ibar VF, Pace ML, McGlathery KJ, Sandoval-Gil JM, Hernández-López J (2016) Resource use of an aquacultured oyster (*Crassostrea gigas*) in the reverse estuary Bahia San Quintin, Baja California, Mexico. Estuaries Coasts 39:866–874

Enríquez S, Duarte CM, Sand-Jensen K (1993) Patterns in decomposition rates among photosynthetic organisms: the importance of detritus C:N:P content. Oecologia 94:457–471

Ezgeta-Balić D, Šantić D, Šegvić-Bubić T, Bojanić N, Bužančić M, Vidjak O, Briski E (2020) Competitive feeding interactions between native *Ostrea edulis* and non-native *Crassostrea gigas* with implications of introducing *C. gigas* into commercial aquaculture in the eastern Adriatic Sea. Mar Environ Res 160:105051

Haag J, Dulai H, Burt W (2023) The role of submarine groundwater discharge to the input of macronutrients within a macrotidal subpolar estuary. Estuaries Coasts 46:1740–1755

Hargrave MS, Nylund GM, Enge S, Pavia H (2022) Co-cultivation with blue mussels increases yield and biomass quality of kelp. Aquaculture 550:737832

Harris D, Horwáth WR, Van Kessel C (2001) Acid fumigation of soils to remove carbonates prior to total organic carbon or carbon-13 isotopic analysis. Soil Sci Soc Am J 65:1853–1856

Hill JM, McQuaid CD (2009) Variability in the fractionation of stable isotopes during degradation of two intertidal red algae. Estuar Coast Shelf Sci 82:397–405

Kamiyama T (2011) Microzooplankton as a food source for

the Pacific oyster *Crassostrea gigas*: seasonal variation in gut contents and food availability. Fish Sci 77:961−974

Kang CK, Choy EJ, Hur YB, Myeong JI (2009) Isotopic evidence of particle size-dependent food partitioning in cocultured sea squirt *Halocynthia roretzi* and Pacific oyster *Crassostrea gigas.* Aquat Biol 6:289−302

Kasim M, Mukai H (2009) Food sources of the oyster (*Crassostrea gigas*) and the clam (*Ruditapes philippinarum*) in the Akkeshi-ko estuary. Plankton Benthos Res 4:104−114

Khalaman VV, Komendantov AY, Golubovskaya NS, Manoylina PA (2021) Comparative efficiency of *Mytilus edulis* as engineering species for shallow-water fouling communities on artificial structures in the White Sea. J Mar Biol Assoc UK 101:511−525

Krumhansl KA, Scheibling RE (2012) Production and fate of kelp detritus. Mar Ecol Prog Ser 467:281−302

Langdon CJ, Newell RIE (1990) Utilization of detritus and bacteria as food sources by two bivalve suspension-feeders, the oyster *Crassostrea virginica* and the mussel *Geukensia demissa.* Mar Ecol Prog Ser 58:299−310

Lehane C, Davenport J (2006) A 15-month study of zooplankton ingestion by farmed mussels (*Mytilus edulis*) in Bantry Bay, Southwest Ireland. Estuar Coast Shelf Sci 67:645−652

Levinton J, Ward J, Shumway S (2002) Feeding responses of the bivalves *Crassostrea gigas* and *Mytilus trossulus* to chemical composition of fresh and aged kelp detritus. Mar Biol 141:367−376

Maberly SC, Raven JA, Johnston AM (1992) Discrimination between ^{12}C and ^{13}C by marine plants. Oecologia 91:481−492

McKinstry CA, Campbell RW, Holderied K (2022) Influence of the 2014−2016 marine heatwave on seasonal zooplankton community structure and abundance in the lower Cook Inlet, Alaska. Deep Sea Res II 195:105012

McMahon KW, Ambrose WG Jr, Reynolds MJ, Johnson BJ, Whiting A, Clough LM (2021) Arctic lagoon and nearshore food webs: relative contributions of terrestrial organic matter, phytoplankton, and phytobenthos vary with consumer foraging dynamics. Estuar Coast Shelf Sci 257:107388

Miller CA, Kelley AL (2021) Seasonality and biological forcing modify the diel frequency of nearshore pH extremes in a subarctic Alaskan estuary. Limnol Oceanogr 66:1475−1491

Miller RJ, Page HM (2012) Kelp as a trophic resource for marine suspension feeders: a review of isotope-based evidence. Mar Biol 159:1391−1402

Park MS, Kim JK, Shin S, Min BH, Samanta P (2021) Trophic fractionation in an integrated multi-trophic aquaculture off Tongyoung Coast: a stable isotope approach. Aquaculture 536:736454

Peterson BJ, Fry B (1987) Stable isotopes in ecosystem studies. Annu Rev Ecol Syst 18:293−320

Post DM (2002) Using stable isotopes to estimate trophic position: models, methods, and assumptions. Ecology 83:703−718

Post DM, Layman CA, Arrington DA, Takimoto G, Quattrochi J, Montana CG (2007) Getting to the fat of the matter:

models, methods and assumptions for dealing with lipids in stable isotope analyses. Oecologia 152:179−189

Rahman MA, Henderson S, Miller-Ezzy PA, Li XX, Qin JG (2020) Analysis of the seasonal impact of three marine bivalves on seston particles in water column. J Exp Mar Biol Ecol 522:151251

Ren JS, Ross AH, Schiel DR (2000) Functional descriptions of feeding and energetics of the Pacific oyster *Crassostrea gigas* in New Zealand. Mar Ecol Prog Ser 208:119−130

Riera P (2007) Trophic subsidies of *Crassostrea gigas, Mytilus edulis* and *Crepidula fornicata* in the Bay of Mont Saint Michel (France): a δ^{13}C and δ^{15}N investigation. Estuar Coast Shelf Sci 72:33−41

Shumway SE, Cucci TL, Newell RC, Yentsch CM (1985) Particle selection, ingestion, and absorption in filter-feeding bivalves. J Exp Mar Biol Ecol 91:77−92

Siegert D, Konar B, Lindeberg MR, Saupe S, Iken K (2022) Trophic structure of key taxa in rocky intertidal communities in two contrasting high-latitude environments. Deep Sea Res II 198:105050

Sosik EA, Simenstad CA (2013) Isotopic evidence and consequences of the role of microbes in macroalgae detritus-based food webs. Mar Ecol Prog Ser 494:107−119

Stabeno PJ, Bond NA, Hermann AJ, Kachel NB, Mordy CW, Overland JE (2004) Meteorology and oceanography of the Northern Gulf of Alaska. Cont Shelf Res 24:859−897

Stekoll MS, Peeples TN, Raymond AE (2021) Mariculture research of *Macrocystis pyrifera* and *Saccharina latissima* in Southeast Alaska. J World Aquacult Soc 52:1031−1046

Stock BC, Semmens BX (2016) MixSIAR GUI user manual, version 3.1. https://github.com/brianstock/MixSIAR

Stock BC, Jackson AL, Ward EJ, Parnell AC, Phillips DL, Semmens BX (2018) Analyzing mixing systems using a new generation of Bayesian tracer mixing models. PeerJ 6:e5096

Strom SL, Olson MB, Macri EL, Mordy CW (2006) Cross-shelf gradients in phytoplankton community structure, nutrient utilization, and growth rate in the coastal Gulf of Alaska. Mar Ecol Prog Ser 328:75−92

Strom SL, Fredrickson KA, Bright KJ (2019) Microzooplankton in the coastal Gulf of Alaska: regional, seasonal and interannual variations. Deep Sea Res II 165:192−202

Ward JE, Shumway SE (2004) Separating the grain from the chaff: particle selection in suspension-and deposit-feeding bivalves. J Exp Mar Biol Ecol 300:83−130

Ward JE, Levinton JS, Shumway SE, Cucci T (1998) Particle sorting in bivalves: *in vivo* determination of the pallial organs of selection. Mar Biol 131:283−292

Xu Q, Yang H (2007) Food sources of three bivalves living in two habitats of Jiaozhou Bay (Qingdao, China): indicated by lipid biomarkers and stable isotope analysis. J Shellfish Res 26:561−567

Xu Q, Gao F, Yang H (2016) Importance of kelp-derived organic carbon to the scallop *Chlamys farreri* in an integrated multi-trophic aquaculture system. Chin J Oceanology Limnol 34:322−329

Yokoyama H, Ishihi Y, Yamamoto S (2008) Diet−tissue isotopic fractionation of the Pacific oyster *Crassostrea gigas.* Mar Ecol Prog Ser 358:173−179

Appendix.

Table A1. Mean (±SD) proportional source contributions of each endmember to the resource use of *Crassostrea gigas* and *Mytilus trossulus* and to the composition of seawater particulate organic matter (POM), separated by sampling month at Spinnaker Sea Farms in Jakolof Bay. The endmembers supplied to the MIXSIAR were macroalgae, phytoplankton, terrestrial organic matter (TOM), and zooplankton. Sampling months covered April, June, August, and December 2023

|	Endmember	April	June	August	December
C. gigas	Macroalgae	0.548 ± 0.069	0.225 ± 0.048	0.578 ± 0.074	0.040 ± 0.070
	Phytoplankton	0.289 ± 0.116	0.000 ± 0.003	0.107 ± 0.122	0.723 ± 0.158
	TOM	0.008 ± 0.022	0.000 ± 0.001	0.015 ± 0.029	0.008 ± 0.023
	Zooplankton	0.154 ± 0.113	0.775 ± 0.048	0.300 ± 0.085	0.229 ± 0.150
M. trossulus	Macroalgae	0.432 ± 0.040	0.248 ± 0.062	0.754 ± 0.038	0.297 ± 0.166
	Phytoplankton	0.545 ± 0.044	0.737 ± 0.079	0.012 ± 0.030	0.457 ± 0.237
	TOM	0.001 ± 0.004	0.009 ± 0.023	0.228 ± 0.032	0.246 ± 0.092
	Zooplankton	0.022 ± 0.025	0.006 ± 0.016	0.007 ± 0.016	0.000 ± 0.001
POM	Macroalgae	0.103 ± 0.066	0.007 ± 0.027	0.011 ± 0.026	0.083 ± 0.098
	Phytoplankton	0.788 ± 0.132	0.026 ± 0.067	0.731 ± 0.137	0.377 ± 0.167
	TOM	0.003 ± 0.016	0.382 ± 0.119	0.002 ± 0.008	0.348 ± 0.074
	Zooplankton	0.105 ± 0.124	0.585 ± 0.134	0.256 ± 0.136	0.192 ± 0.138
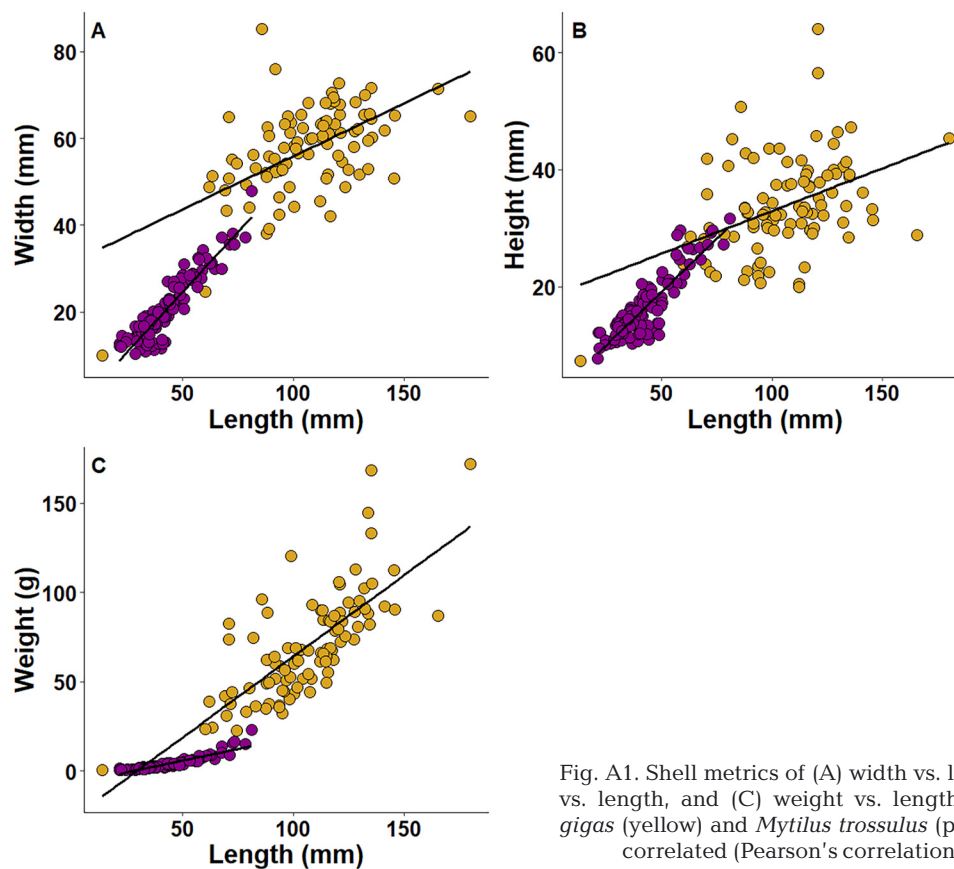
Fig. A1. Shell metrics of (A) width vs. length, (B) height vs. length, and (C) weight vs. length for *Crassostrea gigas* (yellow) and *Mytilus trossulus* (purple) are highly correlated (Pearson's correlation, p < 0.001)